

# Electron states in the quantum wire with periodic serial structure

Jarosław Kłos\*

Surface Physics Division, Faculty of Physics,  
Adam Mickiewicz University,  
ul.Umultowska 85, 61-614 Poznań, Poland  
(Dated: February 6, 2008)

A model quantum wire embedded in a matrix permeable to electron waves is investigated in terms of electronic states. The wire is assumed to have a 1D crystal structure. Through electron waves propagating in its surroundings, lateral modes are coupled with Bloch waves propagating along the wire axis, which results in modes splitting into multiplets. The results presented in this study have been obtained by direct solution of the Schrödinger equation in the effective mass approximation.

## I. INTRODUCTION

Having become the subject of intensive research<sup>1,2,3,4</sup>, electron transport in quantum wires includes an interesting problem of transport in wires showing structural periodicity, which can be due to material composition or geometry variations<sup>5</sup>. A periodic quantum wire can be regarded as a quasi one-dimensional crystal; transmission through it depends on the crystal band structure as well as on open lateral modes.

A more general treatment of the problem to be dealt with here can be found in a paper by Kohn<sup>6</sup> and in later studies<sup>7,8,9</sup>, in which electronic states in crystalline thin films (composed of just a few atomic layers) are investigated by means of the Green's function formalism. In the 1990s, in connection with the possibility of fabricating complex semiconductor heterostructures with molecular beam epitaxy (MBE) technology, papers on electronic properties of quantum wires began to appear. A relatively low percentage of these studies deals with periodic quantum wires, though<sup>10,11,12</sup>. In particular, the problem of electronic state existence in a periodic quantum wire embedded in a permeable medium has not yet been studied thoroughly enough.

The model of quantum wire considered in this paper shows structural periodicity due to variations in material composition, and reflected by periodic variations of the effective mass, as well as of the effective potential felt by electrons moving along the wire axis. The potential confining the electron motion to the wire axis is assumed to be of finite value; consequently, the electron waves do not form nodes on the wire borders and thus can penetrate into the matrix in which the wire is embedded.

The following is implied by the periodicity of the wire structure and the finite potential value in the matrix:

- The electron motion in space cannot be regarded as a superposition of two independent motions, one along the wire axis, the other perpendicular to it. This is why modes localized in the wire form multiplets. Each multiplet is determined by the number of nodes of the envelope function,  $\Psi(y)$ , in the wire, and each mode in a multiplet corresponds to a different Fourier component of Bloch wave  $\Psi(x)$ .
- In spite of the finite value of the potential limit-

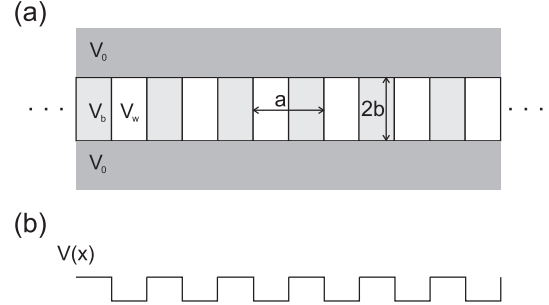


FIG. 1: (a) A schematic representation of a periodic quantum wire composed of alternating segments of  $Al_xGaAs_{1-x}$  (potential barriers) and  $GaAs$  (potential wells). The wire is embedded in an  $AlAs$  matrix. (b) The conduction band bottom level along the wire axis.

ing the electron motion perpendicular to the wire axis, the number of multiplets is infinite. This is due to the reduction of the wave vector (referring to the electron motion along the wire axis) to the first Brillouin zone, which means that even for high energy values corresponding bound states exist in the quantum wire.

The discussed model is based on the effective mass approximation, which, though not applicable when the electron energy is far from the conduction band bottom level, through simplifications made, allows a clear description of conditions of mode existence in a periodic quantum wire.

## II. MODEL

The system to be considered is schematically depicted in Fig. 1. A periodic quantum wire can be regarded as a superlattice with two surfaces close to each other and perpendicular to its layers. The wire is composed of alternating segments of  $GaAs$  and  $Al_xGaAs_{1-x}$ , and embedded in an  $AlAs$  matrix.

The electron motion with energy values close to the conduction band bottom is described by the effective

mass equation:

$$\left[ \frac{\hbar^2}{2} \nabla \frac{1}{m^*(\mathbf{r})} \nabla + E - V(\mathbf{r}) \right] \Psi(\mathbf{r}) = 0. \quad (1)$$

Since the system is homogeneous along the  $z$ -axis, the electron motion described in (1) can be regarded as a superposition of two motions, one taking place in the  $x, y$ -plane, the other being a free motion along the  $z$ -axis. If the latter motion is neglected ( $k_z = 0$ ), the system can be regarded as two-dimensional.

A further factorization of  $\Psi(x, y)$  is possible within the quantum wire:  $\Psi_I(x, y) = \Psi_I(x) \Psi_I(y)$ , with the following differential equations to be satisfied by components  $\Psi_I(x)$  and  $\Psi_I(y)$ :

$$\left[ \frac{\hbar^2}{2m_0} \frac{\partial}{\partial x} \frac{1}{M(x)} \frac{\partial}{\partial x} + E - V(x) - \frac{1}{M(x)} \lambda \right] \Psi_I(x) = 0, \quad (2)$$

$$\left[ \frac{\hbar^2}{2m_0} \frac{\partial^2}{\partial y^2} + \lambda \right] \Psi_I(y) = 0, \quad (3)$$

where  $M(x) = m^*(x)/m_0$ , and  $\lambda$  is the separation constant. The solution,  $\Psi_I(x, y)$ , has the following form:

$$\Psi_I(x, y) = u(x) e^{ixq} e^{i\kappa y}, \quad (4)$$

where  $u(x)$  denotes the periodic factor of the Bloch function, and  $\kappa = \sqrt{\frac{2m_0}{\hbar} \lambda}$ .

Throughout the system, a solution of (1) must fulfill the conditions of continuity at the border between the quantum wire  $I'$  and the matrix  $II'$ :

$$\left. \frac{\partial \Psi_I(x, y)}{\partial x} \right|_{y=\pm b} = \left. \frac{\partial \Psi_{II}(x, y)}{\partial x} \right|_{y=\pm b}, \quad (5)$$

$$\frac{1}{M(x)} \left. \frac{\partial \Psi_I(x, y)}{\partial y} \right|_{y=\pm b} = \frac{1}{M} \left. \frac{\partial \Psi_{II}(x, y)}{\partial y} \right|_{y=\pm b}, \quad (6)$$

where  $M(x)$  and  $M$  denote the relative effective mass in the wire and beyond it, respectively.

For condition (5) to be fulfilled by the wave function beyond the wire,  $\Psi_{II}(x, y)$ , for any  $x$  value, the function must have the following form:

$$\Psi_{II}(x, y) = \sum_{n=-\infty}^{\infty} c_n e^{i(q+Q_n)x} f_n(y), \quad (7)$$

$c_n$  denoting Fourier coefficients of the periodic factor of the Bloch function,  $\Psi_I(x)$ .

$$u(x) = \sum_{n=-\infty}^{\infty} c_n e^{iQ_n x}. \quad (8)$$

The fulfillment of (5) for any  $x$  implies the following boundary conditions for  $f_n(y)$ :

$$f_n^+(y) |_{y \rightarrow \infty} = f_n^-(y) |_{y \rightarrow \infty} = 0. \quad (9)$$

The boundary condition:

$$f_n^+(b) = f_n^-(-b) = 1 \quad (10)$$

means a requirement of mode localization at the wire axis. Superscripts  $'+'$  and  $'-'$  in (9) and (10) refer to the solutions in two half planes, defined by  $y > b$  and  $y < -b$ , respectively.

By including (7) into (1), we get:

$$\sum_{n=-\infty}^{\infty} c_n e^{i(q+Q_n)x} \times \left[ \frac{\partial^2}{\partial y^2} - (q + Q_n)^2 + \frac{2M}{\hbar^2} (E - V_0) \right] f_n(y) \equiv 0, \quad (11)$$

where  $V_0$  is the conduction band bottom level in the matrix. This leads to the following system of differential equations for  $f_n(y)$  with boundary conditions (9) and (10):

$$\left[ \frac{\partial^2}{\partial y^2} - (q + Q_n)^2 + \frac{2M}{\hbar^2} (E - V_0) \right] f_n(y) = 0. \quad (12)$$

The solution of (12) has the form:

$$f_n^{\pm}(z) = e^{\mu_n(z \mp b)}, \quad (13)$$

where

$$\mu_n = \sqrt{(q + Q_n)^2 + \frac{2M}{\hbar^2} (V_0 - E)}. \quad (14)$$

A general solution of (3) is a linear combination of functions:  $C_1 e^{-\kappa y} + C_2 e^{\kappa y}$ . The symmetry of the system allows independent matching of modes that are symmetric or antisymmetric with respect to the wire axis. Thus, the solution of (6) can be found by independent mode matching at one surface only ( $y = b$ ):

$$\frac{1}{M} \kappa \tan(\kappa b) = \frac{1}{M(x)} \frac{\sum_n \mu_n c_n e^{(q+Q_n)x}}{\sum_n c_n e^{(p+Q_n)x}}, \quad (15)$$

$$\frac{1}{M} \kappa \cot(\kappa b) = -\frac{1}{M(x)} \frac{\sum_n \mu_n c_n e^{(q+Q_n)x}}{\sum_n c_n e^{(p+Q_n)x}}. \quad (16)$$

Equations (15) and (16) refer to symmetric and antisymmetric modes, respectively.

In the vicinity of the conduction band bottom the effective mass is a linear function of the band bottom level,  $V(x)$ :

$$M(x) = A + BV(x). \quad (17)$$

Being a periodic function ( $V(x + na) = V(x)$ ), potential  $V(x)$  can be Fourier-expanded:

$$V(x) = \sum_{n=-\infty}^{\infty} v_n e^{iQ_n x}. \quad (18)$$

With only the most significant component of the sum in (18) taken into account,  $M(x)$  is approximately represented by its mean value:

$$M(x) \approx \overline{M(x)} = A + Bv_0. \quad (19)$$

By including this approximation into (15) and (16), we get the following form of the two equations:

$$\sum_{n=-\infty}^{\infty} c_n e^{i(q+Q_n)x} \left( M\mu_n - \overline{M(x)}\kappa \tan(\kappa b) \right) = 0, \quad (20)$$

$$\sum_{n=-\infty}^{\infty} c_n e^{i(q+Q_n)x} \left( M\mu_n + \overline{M(x)}\kappa \cot(\kappa b) \right) = 0. \quad (21)$$

to be satisfied for any  $x$  (i.e. throughout the length of the border between the wire and the matrix). This condition is fulfilled when:

$$M\mu_n - \overline{M(x)}\kappa \tan(\kappa b) = 0, \quad (22)$$

$$M\mu_n + \overline{M(x)}\kappa \cot(\kappa b) = 0. \quad (23)$$

The values of  $\kappa$  corresponding to known energy values  $E$  can be found from (22) and (23). In the limit case, when the matrix is impermeable to electron waves ( $V_0 \rightarrow \infty$ ),  $\kappa$  takes values  $\kappa_l = l\pi/(2b)$ ; odd  $l$  values correspond to modes that are symmetric with respect to the wire axis, and even  $l$  values to antisymmetric ones. Then, wave propagation along the wire axis takes place in effective potential:

$$U(x) = V(x) + \frac{2m^*(x)}{\hbar} l\pi/(2b). \quad (24)$$

When the potential in the matrix is finite, each  $n$  corresponds to a mode multiplet. Each mode in a multiplet corresponds to a different Fourier component of electron wave  $\Psi(x)$ , and involves the fulfillment of condition:

$$(q + Q_n)^2 + \frac{2M}{\hbar^2} (V_0 - E) > 0. \quad (25)$$

Note that modes corresponding to the lowest Fourier components ( $n = 0, \pm 1, \pm 2, \dots$ ) will be successively eliminated from multiplets with increasing energy. As a consequence of (14), (22) and (23), the limit value of  $\kappa$  for  $|n| \rightarrow \infty$  is  $l\pi/(2b)$  in each multiplet.

### III. RESULTS

The calculations performed refer to a quantum wire composed of alternating  $GaAs$  and  $Al_{0.35}GaAs_{0.65}$  segments, representing potential wells and barriers, respectively. The wire is embedded in a uniform homogeneous  $AlAs$  matrix. The energy reference level ( $E = 0$ ) is assumed to coincide with the conduction band bottom in an  $Al_{0.35}GaAs_{0.65}$  barrier. The wells and barriers are assumed to be of equal width,  $40 \text{ \AA}$ . The width of the

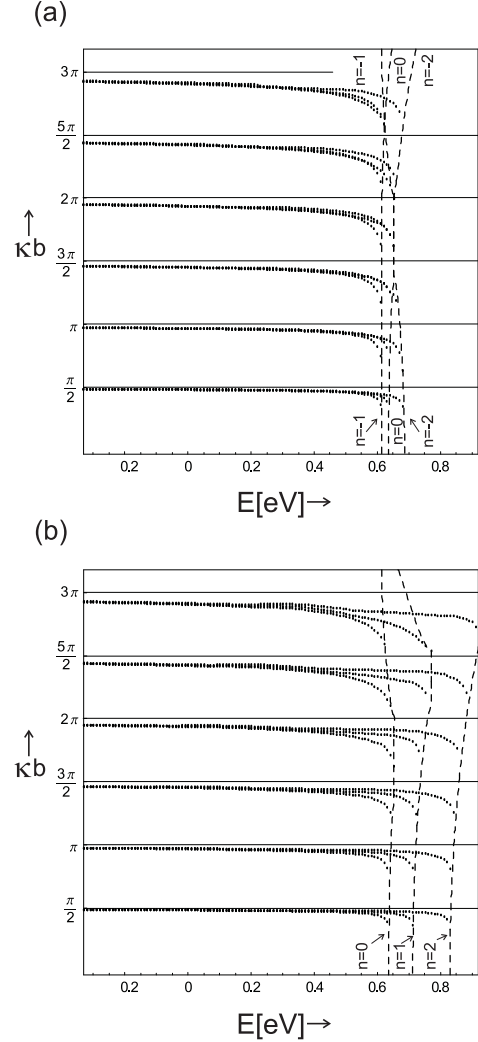


FIG. 2: Parameter  $\kappa_{l,n}$  plotted versus energy for modes (a)  $n = 0, -1, -2$  and (b)  $n = 0, 1, 2$ . Dots represent calculation points; horizontal lines indicate values approached by  $\kappa_{l,n}$  when  $n \rightarrow \pm\infty$  for the first six multiplets,  $l = 1, 2, \dots, 5$ ; dashed lines indicate cut-off energy values.

quantum wire is assumed to be constant throughout its length, and to equal  $200 \text{ \AA}$ .

The values of  $\kappa_{l,n}$  corresponding to localized modes with different energy values have been found from (22) and (23). Subscript  $l$  refers to the number of  $\Psi(y)$  nodes in the quantum wire ( $l = 1, 2, 3, \dots$  corresponds to  $0, 1, 2, \dots$  nodes, respectively). Subscript  $n$  refers to the  $n$ -th Fourier component of Bloch function  $\Psi(x)$ .

Fig. 2 shows  $\kappa_{l,m}$  plotted against electron energy. For clarity reasons,  $\kappa_{l,m}$  values are expressed in units of  $1/b$ ,  $b$  denoting the half-width of the wire. Values  $\kappa b = \pi/2, 3\pi/2, 5\pi/2, \dots$  ( $\kappa b = \pi, 2\pi, 3\pi, \dots$ ) correspond to symmetric (antisymmetric) closed-end modes (with nodes at the wire borders), and to  $n \rightarrow \pm\infty$ . The calculations have been performed for the first five Fourier components  $n = 0, \pm 1, \pm 2$ . The  $\kappa_{l,n}$  values correspond-

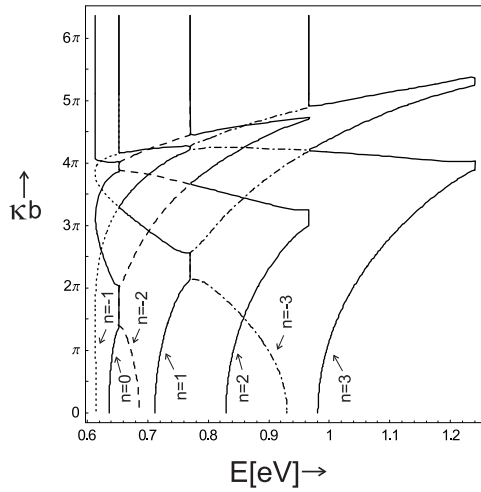


FIG. 3: Parameter  $\kappa$  plotted versus cut-off energy for different modes. Each curve corresponds to a different mode number,  $n$ .

ing to modes in the same multiplet (i.e. having the same number of nodes, or  $l$ ) begin to differ significantly at higher electron energy values. The splitting is also found to grow in extent with increasing  $l$ . The dashed lines in the plot represent the 'cut-off energy' values, at which, in accordance with (25), modes corresponding to successive Fourier components ( $n = 0, \pm 1, \pm 2, \pm 3, \dots$ ) are eliminated as the electron energy increases. In Fig. 3,  $\kappa$  is plotted versus cut-off energy for different modes (different  $n$  values). For high  $\kappa$  values  $q(\kappa, E) = 0$ , and according to (25), the cut-off energy for modes only differing in sign of  $n$  is identical. The variations of cut-off energy for lower  $\kappa$  values are a consequence of the variability of  $q(\kappa, E)$ .

According to (2) and (4),  $\kappa_{l,n}$  defines the effective potential for an electron moving along the wire in mode  $(l, m)$ :

$$U(x) = V(x) + \frac{\hbar^2}{2m^*(x)} \kappa_{l,n} b. \quad (26)$$

At low electron energy values  $\kappa_{l,m}$  remains constant. Therefore, the dispersion relation,  $q(E, \kappa_{l,n})$  (for the motion along the wire), is shifted along the energy axis, the extent of the shift depending on  $\kappa$ . Only at higher energy values, in the range in which mode elimination occurs, the shape of the dispersion curve is found to be significantly changed. Fig. 4 shows the dispersion relation,  $q(E, \kappa_{2,n})$ , for the second multiplet. The solid lines represent dispersion curves for the lowest modes ( $n = 0, \pm 1, \pm 2, \pm 3$ ) in the multiplet. The dashed lines

represent the dispersion curve for an infinite semiconductor superlattice ( $b \rightarrow \infty, \kappa \rightarrow 0$ ).

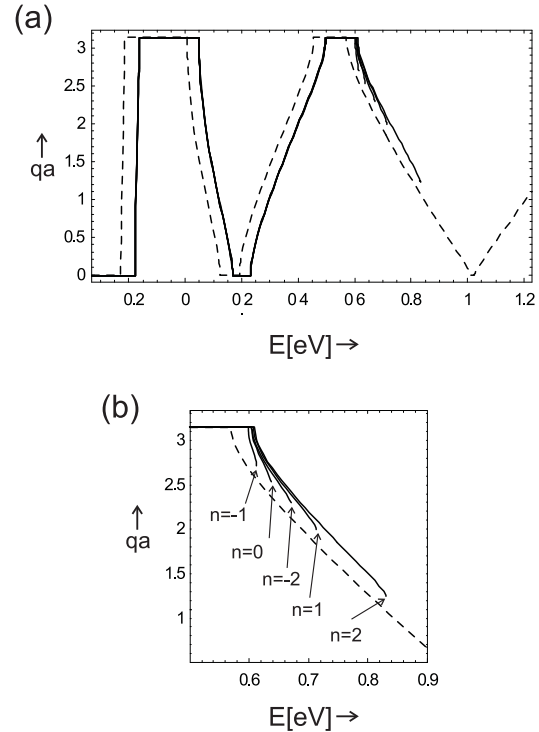


FIG. 4: Dispersion curves for the second ( $l=2$ ) multiplet of modes. Plotted for reference, the respective dispersion curve for an infinite superlattice ( $b \rightarrow \infty$ ) is represented by the dashed line. (b) The area of elimination of modes  $n = 0, \pm 1, \pm 2$  shown in close-up.

#### IV. CONCLUSIONS

Localized electronic modes in a periodic quantum wire ( $\Psi(x, y) \rightarrow 0$  for  $y \rightarrow \pm\infty$ ) are defined by two quantum numbers: (1)  $l$ , referring to the number of nodes of the envelope function in the direction perpendicular to the wire axis; and (2)  $n$ , denoting the number of the corresponding Fourier component of the wave propagating along the wire.

The dispersion curve,  $q(E, \kappa_{l,m})$ , corresponding to each mode multiplet (fixed  $l$ ) is shifted along the energy axis towards higher energy values with respect to the dispersion curve corresponding to an infinite superlattice ( $b \rightarrow \infty$ ). The relative shift of the  $q(E, \kappa_{l,n})$  curve corresponding to individual modes (differing in  $n$ ) in a multiplet remains minor as long as the electron energy is low (i.e. the left-hand side of (25) is much greater than zero); not until the energy gets close to the cut-off value does the mode splitting become noticeable.

\* Electronic address: klos@amu.edu.pl

<sup>1</sup> R. Crook, J. Prance, K.J. Thomas, S.J. Chorley, I. Farrer,

- D.A. Ritchie, M. Pepper, C.G. Smith, *Science* **312**, 1359 (2006)
- <sup>2</sup> M.J. Gilbert, R. Akis, D.K. Ferry, *J. Phys.: Conf. Ser.* **35**, 219 (2006)
- <sup>3</sup> M. Lee, C. Bruder, *Phys. Rev. B*, **72**, 045353 (2005)
- <sup>4</sup> S. Bellucci, P. Onorato, *Phys. Rev. B*, **73**, 045329 (2006)
- <sup>5</sup> J.O. Vasseur, A. Akjouj, L. Dobrzyński, B. Djafari-Rouhani, E.H. El Boudouti, *Surf. Sci. Rep.*, **54**, 1 (2004)
- <sup>6</sup> W. Kohn, *Phys. Rev. B*, **11**, 3756 (1974)
- <sup>7</sup> H. Krakauer, M. Posternak, A.J. Freeman, *Phys. Rev. B*, **19**, 1706 (1979)
- <sup>8</sup> N. Kar, P. Soven, *Phys. Rev. B*, **11**, 3761 (1975)
- <sup>9</sup> O. Jepsen, J. Madsen, O.K. Andersen, *Phys. Rev. B, Phys. Rev. B*, **18**, 605 (1977)
- <sup>10</sup> Yu-Ming Lin, M.S. Dresselhaus, *Phys. Rev. B*, **68**, 075304 (2003)
- <sup>11</sup> L. Piraux, J.M. George, J.F. Despres, C. Leroy, E. Ferain, R. Legras, K. Ounadjela, A. Fert, *Appl. Phys. Lett.*, **65**, 2484 (1994)
- <sup>12</sup> M.P. Persson, H.Q. Xu, *Phys. Rev. B*, **73**, 035328 (2006)